Geophysical Research Letters

RESEARCH LETTER
10.1029/2018GL079968

**Key Points:**
- We assess downward carbon flux temporal evolution along the season from simulated sinking carbon and dissolved and particulate $^{234}$Th depth profiles
- We analyze the accuracy of the steady/non-steady state approaches to calculate the $^{234}$Th-derived carbon flux in relation to the trap flux
- We quantify temporal windows during which the steady state approach results accurate and introduce the concept of "window of success"

**Supporting Information:**
- Supporting Information S1
- Data Set S1

**Correspondence to:**
E. Ceballos-Romero,
eceballos1@us.es

**Citation:**
Ceballos-Romero, E., De Soto, F., Le Moigne, F. A. C., García-Tenorio, R., & Villa-Alfageme, M. (2018). $^{234}$Th-derived particle fluxes and seasonal variability: When is the SS assumption reliable? Insights from a novel approach for carbon flux simulation. *Geophysical Research Letters*, *45*, 13,414–13,426. https://doi.org/10.1029/2018GL079968

Received 10 AUG 2018
Accepted 28 NOV 2018
Accepted article online 3 DEC 2018
Published online 29 DEC 2018

©2018. American Geophysical Union. All Rights Reserved.

# $^{234}$Th-Derived Particle Fluxes and Seasonal Variability: When Is the SS Assumption Reliable? Insights From a Novel Approach for Carbon Flux Simulation

**E. Ceballos-Romero[1], F. De Soto[2], F. A. C. Le Moigne[3,4], R. García-Tenorio[1], and M. Villa-Alfageme[1]**

[1]Departamento de Física Aplicada II, Universidad de Sevilla, Seville, Spain, [2]Departamento de Sistemas Físicos, Químicos y Naturales, Universidad Pablo de Olavide, Seville, Spain, [3]GEOMAR Helmholtz Centre for Ocean Research Kiel, Kiel, Germany, [4]Mediterranean Institute of Oceanography (MIO), UM110 (CNRS/INSU, Aix-Marseille Université, IRD), Marseille, France

**Abstract** $^{234}$Th measurements are widely used to estimate the downward carbon flux of particles via the oceanic Biological Pump. Carbon export is evaluated from $^{234}$Th-$^{238}$U disequilibrium assuming either steady state (SS) conditions, or including a non-SS (NSS) correction. We use a novel stochastic simulation to quantify the temporal variation of vertical carbon and $^{234}$Th (dissolved and particulate) concentration profiles with high temporal resolution. We calculate seasonal export as if in situ measured with sediment trap and SS- and NSS-$^{234}$Th approaches and quantify the periods of validity for SS/NSS conditions defined in previous works. The SS approach is valid throughout the entire season in oligotrophic regions. In temperate regions, the SS introduces a bias in the export if sampling takes place outside specific temporal windows. Windows of validity range from days in short blooms of ~15-day duration to weeks in blooms longer than ~30 days.

**Plain Language Summary** Climate change driven by anthropogenic $CO_2$ emissions has a significant impact on mankind. An important component of Earth's carbon cycle is the ocean's biological carbon pump (BCP), which buffers the air-sea balance of $CO_2$. It starts with production of organic matter in the surface ocean, continues with its sinking into the dark ocean, and finishes with the storage of a small fraction below 1,000 m. Without the BCP, atmospheric $CO_2$ concentration would be 50% higher than it currently is. Understanding the BCP helps to predict the future $CO_2$ that will be stored by the oceans and how that will affect the global carbon cycle. The photosynthetically fixed carbon is mainly transferred as large particles. Among the methods currently used to estimate the downward flux of particles, sediment traps, and $^{234}$Th-$^{238}$U radioactive pair are the most accepted ones. However, the simultaneous use of these two techniques does not always provide comparable flux estimates. This questions the consistency of our current calculations of the magnitude of the carbon flux and the accuracy of the global predictions. In this study, we assess the accuracy of the $^{234}$Th method in relation to the traps and explain the source of the discrepancies between them.

## 1. Introduction

Carbon export and sequestration result from a large variety of biological, ecological, physical, and chemical processes (Ducklow et al., 2001). The mechanisms of the biological pump (BP; Volk & Hoffert, 1985) are responsible for transforming dissolved inorganic carbon into organic biomass and pumping it into the deep ocean. The capability of the oceans to export and store carbon via the BP are ultimately controlled by the production, transport, and destruction of particles (Passow et al., 2006) and influences global atmospheric $CO_2$ levels (Kwon et al., 2009). Accurate estimates of the magnitude of the BP and carbon export fluxes are therefore key to improve our predictions of the ocean's carbon uptake.

In situ techniques have been widely used to evaluate particle fluxes and the efficiency with which particulate organic carbon (POC) is exported from the surface ocean (Buesseler, 1998). Our current knowledge of the magnitude of carbon export fluxes relies on a spatially and temporally limited number of field measurements, mostly based on sediment traps (both tethered and, more recently, Lagrangian neutrally buoyant NBST - Neutrally Buoyant Sediment Trap - and PELAGRA- Particle Export measurement using a LAGRAngian trap - types; Buesseler, Trull, et al., 2008; Buesseler et al., 2007; Lamborg et al., 2008; Lampitt et al., 2008; Marsay et al., 2015; Owens et al., 2013), and radioactive pairs (mainly $^{234}$Th; Buesseler et al., 1998; Ceballos-Romero

et al., 2016; Le Moigne, Villa-Alfageme, et al., 2013; Roca-Martí et al., 2015; Rutgers van der Loeff et al., 1997; Stewart et al., 2011; Verdeny et al., 2009). However, the simultaneous use of traps and $^{234}$Th method does not always provide consistent estimates (e.g., Verdeny et al., 2009; Stewart et al., 2011; Ceballos-Romero et al., 2016) and questions the consistency of our current estimates of the magnitude of the carbon export flux.

### 1.1. Steady State Versus the Non-Steady State Assumptions

Measurements are frequently limited by single-time samplings of the study sites due to difficulties in cruise programming and time restrictions, so the assessment of $^{234}$Th activity gradients in time or space is challenging. It is thus necessary to assume simplifications in the sampling conditions, such as neglecting changes in $^{234}$Th concentrations over time—the so-called steady state (SS)—to compute $^{234}$Th flux (Buesseler et al., 1992). Along with other factors, the SS assumption has been repeatedly acknowledged as a source of uncertainties and discrepancies with sediment trap results since the beginning of the use of the method (e.g., Buesseler et al., 1992, 1998; Buesseler, Lamborg, et al., 2008; Maiti et al., 2008; Rutgers van der Loeff et al., 1997; Savoye et al., 2006). $^{234}$Th cannot trace fast exports events because deficits unavoidably persist in the water column according to its half-life (i.e., 24.1 days). This is crucial for the evaluation of the export using $^{234}$Th measurements (Amiel et al., 2002).

A large proportion of the ocean exhibits variability in the export within the half-lives of the radionuclides (Henson et al., 2015) and the SS assumption may not be always valid. The consequences of using the SS approach to obtain $^{234}$Th-derived POC fluxes (Th-POC hereafter) has been extensively discussed. The seminal work of Buesseler et al. (1992) showed that temporal change in $^{234}$Th activity might be an important term in the budget and claimed that the SS assumption underestimates $^{234}$Th removal in periods of intense scavenging, while overestimates it during postbloom conditions. Subsequent studies have proposed that assuming SS conditions is only accurate when the production varies slowly in time scales of $^{234}$Th half-life (Buesseler et al., 1992; Savoye et al., 2006) so the SS approach might introduce a systematic bias (Buesseler, Lamborg, et al., 2008; Maiti et al., 2009). In fact, studies from Buesseler et al. (1995) and Maiti et al. (2008) clearly showed that $^{234}$Th cannot always be systematically assumed to be in SS. According to Rutgers van der Loeff et al. (1997) and Savoye et al. (2006), the SS approximation could yield to overestimate (underestimate) $^{234}$Th fluxes by a factor of 6–7.

Quantification of the accuracy of the SS assumption applied to $^{234}$Th profiles on the export estimate is very rarely done since it requires a precise knowledge of the evolution of $^{234}$Th deficits over time. A non-SS (NSS) approach provides an alternative way to interpret $^{243}$Th deficits that accounts for the temporal changes in $^{234}$Th concentration. It is based on the difference between two successive profiles (Buesseler et al., 1992). When repeated sampling at the study area is possible, and uncertainties associated to the $^{234}$Th concentration measurements are small enough, the temporal change of $^{234}$Th concentration can be accounted for by including a linear correction to the SS solution (Buesseler et al., 2005). However, the NSS approximation does not always guarantee a better estimate than the one obtained with the SS approximation due, for example, to high uncertainties obtained mainly due to physical effects (i.e., heterogeneity of water masses and advective and diffusive influences; Resplandy et al., 2012). If the differences in $^{234}$Th concentrations are relatively low, the export estimate would have a high uncertainty (Friedrich & Rugters van der Loeff, 2002). The key issue for the success of the NSS approach relies on the time scale between the reoccupations (Savoye et al., 2006; Stukel et al., 2015). Savoye et al. (2006) thoroughly examined the assumptions behind both SS and NSS $^{234}$Th flux model and recommended reoccupations of the sampling sites from 1 to 4 weeks after first occupation.

Overall, partly due to the fact that it is very often the only possible choice, the most widely used approach to estimate the downward $^{234}$Th flux is a simple one-box-SS model of $^{234}$Th uptake (detailed elsewhere, e.g., Buesseler, 1998; Savoye et al., 2006) in which contributions due to horizontal and vertical advection and diffusion process of the dissolved $^{234}$Th are generally neglected (e.g., Ceballos-Romero et al., 2016; Le Moigne, Villa-Alfageme, et al., 2013; Roca-Martí et al., 2015; Stewart, Cochran, Miquel, et al., 2007) or quantified and found negligible (e.g., Morris et al., 2007). The majority Th-POC export estimates available are calculated under these idealized conditions where the deficit of $^{234}$Th is exclusively due to the downward flux of $^{234}$Th resulting from sinking particles scavenging (see review by Le Moigne, Henson, et al., 2013, and more recently, studies by, e.g., Ceballos-Romero et al., 2016; Le Moigne et al., 2015, 2016; Owens et al., 2015;

Planchon et al., 2015; Puigcorbé et al., 2017; Roca-Martí et al., 2015; Rosengard et al., 2015). Present global carbon databases might therefore correspond to biased estimates of the carbon export. This likely compromises our estimates of the global strength of the BP (Henson et al., 2011) and partly accounts for the inconsistencies reported in the global carbon budgets (Burd et al., 2010; Giering et al., 2014).

### 1.2. Our Numerical Approach

Addressing the correct interpretation of the current Th-POC flux estimates requires a quantitative comprehension of the SS and NSS approaches and the possible bias introduced by their use. Only a few studies have considered the possible effect of nonsteadiness on the export (Amiel et al., 2002; Benitez-Nelson et al., 2001; Buesseler et al., 1992, 1998; Coppola et al., 2005; Friedrich & Rugters van der Loeff, 2002; Gustafsson et al., 2004; Resplandy et al., 2012; Rutgers van der Loeff et al., 1997; Savoye et al., 2004, 2006; Wei & Murray, 1992). Comparisons between SS and NSS solutions have generally reported NSS estimates higher relative to SS ones early in the bloom, while the opposite behavior in periods of export declination (Amiel et al., 2002; Benitez-Nelson et al., 2001; Buesseler et al., 1992; Savoye et al., 2006). Some other studies have found good agreement between estimates (Coppola et al., 2005; Gustafsson et al., 2004).

A thorough comparison between both approaches is nonetheless limited by the insufficient in situ time series data to apply a NSS model. Previous discussions on the topic can be therefore improved with the use of mathematical tools to quantify the vertical and temporal evolution of $^{234}$Th activities. The novelty of this work is the use of a novel approach based on stochastic simulations to couple particle dynamics and radioisotope scavenging in ocean waters by using time-dependent functions. Thereby, this method allows us to study transient regimes by means obtaining outputs over time for any time scale of interest (de Soto et al., 2018) and quantify the SS/NSS issue through comparing the SS and NSS export estimates with the actual carbon flux.

Here four simplified bloom scenarios with contrasted temporal variability are used to obtain the time series vertical concentration of sinking carbon and $^{234}$Th (both dissolved and particulate) along the season. From these outputs, we evaluate carbon export flux during the season in three different ways: (i) directly from the simulated carbon concentration as the total carbon sinking flux, as done in situ with sediment traps (e.g., Lampitt et al., 2008), and indirectly from the simulated $^{234}$Th-$^{238}$U disequilibrium, as done with the $^{234}$Th, using both (ii) SS and (iii) NSS approaches. We assess the impact of interpreting $^{234}$Th deficits assuming SS conditions and applying an NSS linear correction by comparing the results with the simulated trap fluxes. From this, we quantify the valid time windows for $^{234}$Th sampling during which is accurate to use the SS/NSS approaches as function of the temporal variability the export. We aim to set general guidelines regarding the periods of validity for SS- and NSS-$^{234}$Th export estimates. This will bring new insights into the discrepancies between trap and radionuclide-based export estimates reported and provides a practical perspective for the correct use of current and future Th-POC export estimates. Finally, we compile and discuss the reliability of $^{234}$Th-based export estimates reported by previous published studies for different biogeochemical settings according to our predictions.

## 2. Methods

### 2.1. Simulation for Seasonal Carbon Flux

The concentration of particles through the ocean is balanced by the production of new particles, mainly in the euphotic zone, their degradation and recycling by biological processes, and their sinking (details, e.g., Burd et al., 2000). Time and depth variations in particles concentration are governed by a continuity equation that relates particle production, sinking, and degradation processes (see, e.g., Kriest & Oschlies, 2008). Models differ in the parametrization of these processes chosen and the way they resolve the continuity equation. Most of them compute the concentration of particles by solving the continuity equation in time and/or depth for time-independent parametrizations of the production and degradation processes (as done in Burd et al., 2000; Marchal & Lam, 2012, among others). As a novelty to previous models, the simulation here employed solves the continuity equation simultaneously both in time and depth and includes an explicit parametrization of the particle production variable over time. Therefore, the simulation allows to study the transient regimes that are not usually included in previous studies (e.g., Burd et al., 2000; Jackson & Burd, 2001;

Marchal & Lam, 2012) and provides an ideal test bed for the study of sampling sites that are not in SS conditions.

#### 2.1.1. Seasonal Particle Dynamics and Radioisotope Scavenging

We simulate particle production, sinking, degradation, and $^{234}$Th scavenging by those particles in the oceans along the season in simplified bloom scenarios. We obtain the evolution of the profiles in depth of the concentration of both sinking carbon and $^{234}$Th (dissolved and particulate) over time. To do so, in the simulation, particles

1. are randomly produced within the mixed layer depth with a depth-dependent probability distribution and a time-variant rate (i.e., production function);
2. are moved to depth with a depth- and time-invariant sinking rate common for all particles;
3. are allowed to interact with dissolved radionuclide and trace metals of interest in a first-order process via effective adsorption/desorption rates;
4. are randomly destroyed with a depth-dependent probability distribution and a time-invariant rate (i.e., degradation function); and
5. the seasonal carbon export curve is built. A temporal decoupling between steps 1 and 4 can be introduced or not depending on the specific case of study (see section 2.1.2).

The implementation of a time-variant production rate is an innovative approach that reproduces the fluctuations occurring during a bloom similarly in the field. It allows to assess the observed seasonal variation in the production of particles and simulate any temporal pattern of the carbon export and obtain the associated $^{234}$Th export along the season.

The equations used to simulate particle dynamics and radionuclide scavenging are shown in the supporting information. A thorough description of the simulation can be found in De Soto et al. (2018). We obtain (i) the depth profile of sinking carbon concentration throughout time ($n(z, t)$) as a result of the iterative application of steps 1, 2, and 4, and the depth profile of $^{234}$Th concentration throughout time in (ii) the dissolved phase ($a^{D}_{Th}(z, t)$) and (iii) the particulate phase ($a^{P}_{Th}(z, t)$) as a result of the iterative application of step 3. Hence, from our simulation we obtain the equivalent concentration profiles to those sampled in situ with traps and $^{234}$Th along the season.

#### 2.1.2. Building the Seasonal Carbon Export Flux Curve

Different approaches and data sets can be used to reproduce the seasonal carbon export curve (see point 5 in the previous section). In this specific study, we chose data from Porcupine Abyssal Plain site (48°N, 16.5°W, PAP site) and use annual time series of satellite-derived chlorophyll *a* (Chl *a*) data to qualitatively establish the temporal dependence of POC export along the season (see point 1 in the previous section). We simplify and assume that the Chl *a* and the primary production (PP) follow the same temporal pattern and implement the function that best fits the annual pattern of Chl *a* concentrations as input for particles production rate. This function defines our production curve and the day from maximum production (DFMP) establish the prebloom and postbloom phases. In our simulations using data from the PAP site, the recognized temporal decoupling between PP and subsequent export is accounted for by following Stange et al. (2016), who estimated average time lags (TLs) of ~7 days in the North Atlantic based on in situ studies in arctic, temperate, and subtropical regions. Therefore, we assumed no delay between production and export. We introduce the concept of day from maximum export (DFME) to distinguish prepeak and postpeak phases and set the day of maximum production of sinking particles as day of maximum export (i.e., DFMP = DFME). This parameter is relevant in the context of our definition of prepeak (postpeak) phases in relation to prebloom (postbloom) conditions (as discussed in section 4).

We assume that the uncertainty of assuming no delay in the built export curve is relatively small in this case given the short TL estimated at the PAP site relative to the typical bloom duration of several weeks in the PAP site (e.g., Le Moigne et al., 2013). Thereby, it is accurate enough to use the variation of Chl *a* annual pattern as guidance to set the progression of the export over time. Nevertheless, note that when necessary, a temporal offset between Chl *a* and export can be numerically added to our simulation.

In other areas, if a significant delay between production and export is expected, the approach used for the PAP site to obtain the export curve is a simplification of a real scenario. However, it does not impair the

assessment of the effect of the SS and NSS approaches in the interpretation of $^{234}$Th data as a function temporal variability of the export.

The TL between production and export changes substantially with ocean region and season, so each case of study must be therefore analyzed independently according to the region under study (Henson et al., 2015; Stange et al., 2016). In ocean regimes with longer TL, for example, ~15 days in latitudes the Grand Bay (27.9°N, 15.4°W; Stange et al., 2016) we need a more realistic representations of the export curve. In those cases, (i) we can reevaluate the export curve based on Chl *a* data and introduce the estimated TL corresponding to the region; (ii) alternatively, when available, we could use time series of in situ measured PP, or export profiles—either in situ measured or extrapolated from previous studies in the region—from other techniques, such as sediment traps, to construct the export curve.

On the other hand, at this stage of the simulation, no changes in the mixed layer depth over time and negligible lateral/vertical advection are included in the water mass where the particles are produced. Although this is a simplification of the $^{234}$Th system since physical supply and loss terms cannot be always considered minimal (Buesseler et al., 1995; Maiti et al., 2008), in many scenarios, it is found that physical terms contribute $<$10% to the overall activity (Buesseler, 1998), especially in open ocean settings (Savoye et al., 2006), and $^{234}$Th flux mainly is driven by its half-life and its scavenging by particles.

The degradation function comprises all the processes that result in the partial or total release of the particulate carbon back to the water (dissolved phases of carbon), such as zooplankton feeding, microbial degradation, and solubilization of particles. For simplicity, it was chosen to be instantaneous rather than gradual, so the action of the degradation function on a particle entirely and instantaneously returns its carbon content back to the dissolved phase and, in practical carbon terms, destroys the particle entirely. The effective adsorption rate accounts for all the processes that result in the conversion of dissolved $^{234}$Th in to its particulate phase and vice versa for the degradation rate.

Our simulated scenario is therefore a simplification of a real complex ecosystem, however, provides the base to further implement more realistic situations that include more complex processes such as multiple particle size, temporally variable degradation and sinking rates, or physical non-SS effects due to circulation (see de Soto et al., 2018), and it serves as a flexible test bed for analyzing the bias introduced when using SS or NSS approaches for Th-POC fluxes evaluation. In actual bloom scenarios where physical effects due to water circulation might play a significant role, the accuracy of the SS/NSS approaches may only be expected to be reduced. We therefore study a best-case scenario with our simplified bloom simulation and acknowledge that the biases for real blooms would be always larger than for this simple case.

#### 2.1.3. Seasonal POC Fluxes

From our simulation, we calculate $^{234}$Th sinking fluxes along the season from the computed $^{234}$Th-$^{238}$U disequilibrium (both assuming SS conditions: $P_{Th}^{SS}$ and applying a linear NSS correction: $P_{Th}^{NSS}$) and convert them to POC fluxes by using the simulated ratio of POC to $^{234}$Th on sinking particles (see, e.g., Ceballos-Romero et al., 2016, for more details). To analyze both approximations in relation to the sampling moment and the bloom stage, $^{234}$Th-derived POC results are compared to the POC flux estimated directly from the sinking carbon.

In detail, by using our three primary computed outputs ($n(z, t)$, $a_{Th}^{D}(z, t)$, and $a_{Th}^{P}(z, t)$) we estimate the daily variation of the POC flux reproducing the three ways POC export is measured by field measurements:

1. Sediment traps:

The POC flux is obtained directly from the computed profiles of sinking carbon concentration—output (i)—as the total amount of carbon that sinks per unit of surface and time at a given depth. In the simplest case of all particles being identical the flux out of the surface is dictated by the sinking speed ($v$):

$$POC_{trap}\ (z,t) = n(z,t)\cdot v. \tag{1}$$

This will be referred as direct-POC flux hereafter.

2. $^{234}$Th technique (single sampling: SS):

The POC flux at a given depth is obtained by converting the $^{234}$Th sinking flux—by using outputs (ii) and (iii)—estimated assuming SS conditions, that is, constant or slowly changing $^{234}$Th concentrations over time:

$$P_{Th}^{SS}(z,t) = \int_0^z \lambda_{Th} \cdot (a_U - a_{Th}) \cdot dz, \quad (2)$$

where $a_U$ is the sea-conservative $^{238}U$ total concentration, calculated from calibrated salinity measurements (Owens et al., 2011), $a_{Th}$ is the simulated $^{234}Th$ total concentration—$a_{Th}^{D}(z,t) + a_{Th}^{P}(z,t)$—and $\lambda_{Th}$ is $^{234}Th$ half-life ($T_{1/2}$ = 24.1 day). This will be referred as SS-POC hereafter.

3. $^{234}Th$ technique (resampling: NSS):

The POC flux at a given depth is obtained by converting the simulated $^{234}Th$ sinking flux—by using outputs (ii) and (iii)—estimated assuming reoccupation of the sampling site after a time gap $\Delta t$, and including an NSS correction for the temporal change of $^{234}Th$ activities:

$$P_{Th}^{NSS}(z,t) = P_{Th}^{SS}(z,t) - \int_0^z \frac{\Delta a_{Th}}{\Delta t} \cdot dz. \quad (3)$$

This will be referred as NSS-POC hereafter.

### 2.2. Experimental Data

Seasonal variation of direct- and Th-POC fluxes are obtained for any biogeochemical setting desired by adjusting the input parameters (see section 2.1.1). In this study, we use the complete data set from the exhaustive sampling at the PAP site that took place on board RRS Discovery in cruise D341 in summer 2009 (Giering et al., 2014; Le Moigne, Villa-Alfageme, et al., 2013; Marsay et al., 2015; Riley et al., 2012; Villa-Alfageme et al., 2014, 2016).

The production function, particle sinking velocities and degradation function parameters were chosen based on the data from Le Moigne, Villa-Alfageme, et al. (2013), Villa-Alfageme et al. (2014, 2016), and Marsay et al. (2015), respectively. A smoothed Gaussian function of 45-day width was used to reproduce the annual pattern of Chl *a* concentration of the PAP site in 2009 (Le Moigne, Villa-Alfageme, et al., 2013; see also Data Set S1 in the supporting information). The effective adsorption/desorption rates for $^{234}Th$ are estimated in de Soto et al. (2018). The details of how all these input parameters were determined are provided in the supporting information.

Finally, data from PELAGRA traps (Lampitt et al., 2008), and $^{234}Th$-derived POC fluxes from several studies that combined both techniques simultaneously to estimate the export (e.g., Ceballos-Romero et al., 2016; Le Moigne, Villa-Alfageme, et al., 2013; Stewart, Cochran, Xue, et al., 2007) were compared to our modeled results (section 4).

## 3. Results and Discussion

### 3.1. Temporal Evolution of Particle Concentration and $^{234}Th$ Deficits

We simulated the daily evolution of the vertical profiles of sinking carbon concentration and associated $^{234}Th$-$^{238}U$ disequilibrium along the season from the period from ~100 day before the maximum export (here referred from now on as prepeak), up to ~180 day after the export starts to decline (here referred hereafter postpeak). The time series simulated profiles are shown in the supporting information (Figure S1).

We found that sinking carbon concentration changes over time keeping pace with the temporal variation of carbon export. However, the time series profiles of $^{234}Th$ deficit increases as the carbon export increases but then persist almost constant for a certain period of time when the export starts to decline. This temporal evolution of $^{234}Th$ activities was emphasized in the first application of $^{234}Th$ deficits for POC flux in the seminal work of Buesseler et al. (1992). This work shows the time series profiles in a high resolution for the first time.

The contrasted reaction of $^{234}Th$ deficits to changes in the carbon export during the prepeak and postpeak export phases is a consequence of the different mechanisms that govern the increase and decrease of $^{234}Th$ deficits (de Soto et al., 2018). The increase of $^{234}Th$ deficits is the result of the adsorption process and the export, both dictated by the particle dynamics. Rapid reactions of sinking carbon concentrations to the increments in carbon export, due to the increase in Chl *a* concentrations, drive rapid reactions of $^{234}Th$ deficits. Therefore, the use of the SS assumption during the prepeak phase must be used with special care, or it may lead to a biased quantification of $^{234}Th$ flux and derived POC flux, as reported by in situ studies (e.g.,

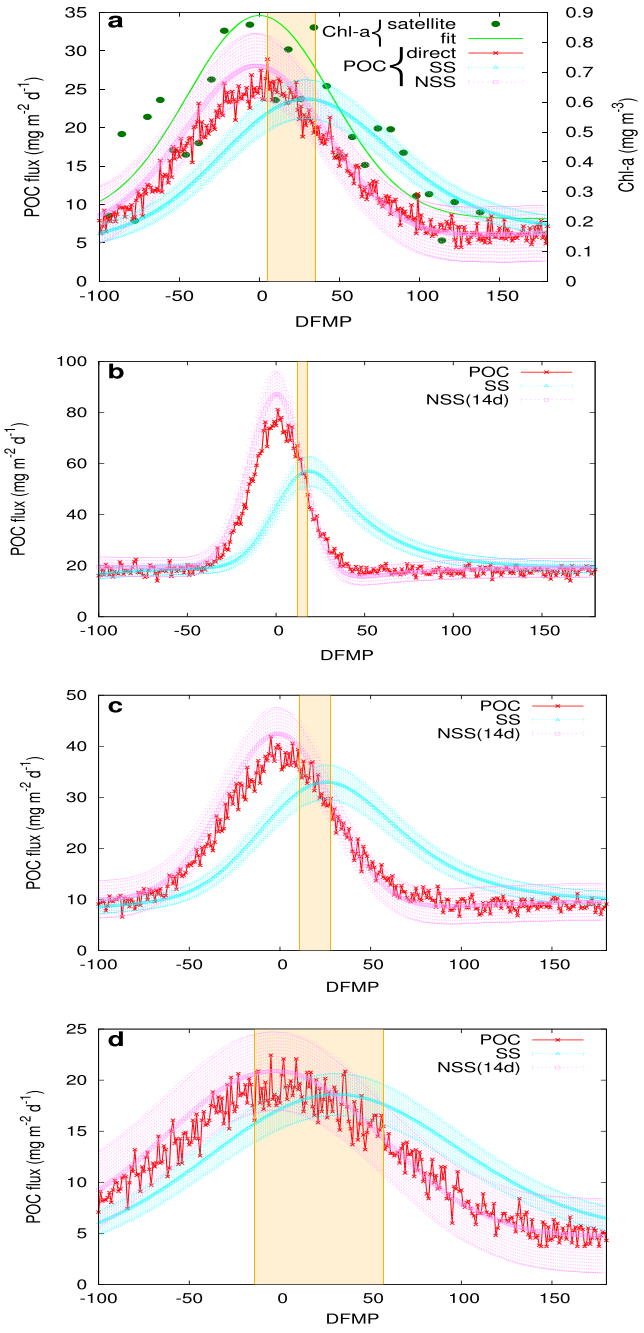


**Figure 1.** (a) Temporal evolution of seasonal direct POC flux and the SS/NSS estimates from 100 days before to 100 days after the maximum production (denoted as DFMP 0). Overall uncertainties associated to both SS and NSS approaches are also marked. Both satellite-derived Chl *a* concentrations and the Gaussian best fit employed to reproduce them were also included (green points and green lines respectively). The shaded box indicates the sampling period during which the SS approach provide consistent results with the direct estimate of the export (the so-called "window of success"). Corresponding plots for blooms reproduced using a production rate that follows a Gaussian function of width of (b) 15 days, (c) 30 days, and (d) 60 days. Chl *a* = chlorophyll *a*; DMFP = day from maximum production; POC = particulate organic carbon; SS = steady state; NSS = non-SS.

Benitez-Nelson et al., 2001; Buesseler et al., 1992). The decrease of $^{234}$Th deficits is controlled by both desorption and degradation processes, along with the radioactive decay of $^{234}$Th itself. The total radioactivity is considered to have disappeared after five half-lives. In the case of $^{234}$Th, this means that the half-life of $^{234}$Th causes the persistence of $^{234}$Th disequilibrium in the water column up to ~120 days. Consequently, despite the decrease of the concentration of sinking carbon, $^{234}$Th concentrations remain approximately constant during a lapse of time ruled by $^{234}$Th half-life and starts changing over time afterward. In our simulation, this implies that, in the postpeak phase, there is a time window of ~40 days during which the assumption of SS conditions to estimate the export with the $^{234}$Th technique is correct, because $^{234}$Th concentration remains fairly constant.

### 3.2. Seasonal Export: Defining "Windows of Success" for Sampling

Figure 1a shows the direct-, SS-, and NSS-POC flux estimates obtained from the time series simulated vertical profiles of sinking carbon concentration and $^{234}$Th deficit following approaches 1–3, respectively (see section 2.1.2), along the entire productive season (from DFME −100 to DFME +180). Note the variability of the direct POC flux estimate, which is characteristic of the stochastic approach, we follow for the creation of sinking mass and can be reduced by incrementing the amount of total sinking mass created per day (de Soto et al., 2018). A quantification of the overall uncertainties was done assuming relative errors of 10% for the main methodological sources of error (i.e., total $^{234}$Th concentration and $^{234}$Th concentration in particles) in order to better reproduce the in situ performance of the $^{234}$Th method (shaded curves).

These seasonal results allow for comparison of the accuracy of the SS and NSS approaches applied to the $^{234}$Th technique in relation to the direct methods and to analyze their reliability to evaluate the POC flux. The SS approach (Figure 1, light-blue lines) successfully predicts the direct-POC flux within uncertainties when the sampling takes place in a specific time frame (Figure 1a, shaded box). This time frame delimits a "window of success" (WOS) to sample for a SS $^{234}$Th analysis that extends after the export peak. Outside from this window, the SS assumption introduces a delay in the export estimate, which yields to an underestimation of the POC flux during the prepeak phase and an overestimation during the postpeak phase.

In the case of a bloom of 45 days of duration that we simulated, the WOS lasts ~30 days, from DFME ~5 to DFME ~35 according to Figure 1a (shaded box). This implies that the SS underestimates the export from DFME −80 to DFME 5 and overestimates it from DFME ~35 to DFME ~130.

A further analysis of the duration and variability of these WOS in terms of the temporal shape of the bloom is carried out in the next section.

Regarding the NSS approach, in case that cruise strategy allows WOS resampling of the stations, it is the most successful solution applied to the $^{234}$Th technique to predict POC export. However, it is important to note that in that case, uncertainties increase due to special variability due to physical events (Resplandy et al., 2012). A balance between the uncertainties associated to the in situ determination of the $^{234}$Th concentration and the temporal changes of $^{234}$Th concentration due to de novo export events has to be considered. Uncertainties may be too large to

accurately measure $^{234}$Th concentration if the resampling takes place too soon. Also, if the time lag between reoccupations increases to time scales larger than local spatial gradients, temporal changes in $^{234}$Th concentration might not be representative of the same water mass of the first sampling (Resplandy et al., 2012) and the linear correction would not be sufficient. Our results suggest that, when reoccupation of the sampling stations takes place within lapses of time between 2 and 3 weeks, an NSS assessment of the export would be accurate (see supporting information, Figure S1). Outside of that reoccupation time, the SS is recommended.

### 3.3. How Does the WOS Change With Bloom Duration?

The duration of the bloom typically ranges from weeks to months and depends on latitude (Cole et al., 2012). The extent of the consequences of assuming SS in $^{234}$Th scavenging models depends on the range of temporal variability (Buesseler et al., 1992). Therefore, the duration of the WOS is expected to rely, among other factors, on the rapidity of the onset/decline of the production periods and on the magnitude/duration of the production (i.e., the temporal variability and intensity of the bloom). We assess here the influence of the temporal pattern (intensity/length) of the bloom on the duration of the WOS.

The width of the Gaussian function used as production rate controls both the magnitude and the rate of changes in the concentration of particles in our simulation (see section 2.2). Scenarios with same productivity (i.e., equal total amount of POC sinking carbon produced along the season) but contrasted bloom duration are reproduced by implementing Gaussian distributions that generate the same total number of particles during the year but with different widths. This is a way of producing blooms of different intensities.

The duration of the WOS increases between sampling frames lasting from ~6 days in short blooms of ~15-day duration (Figure 1b), ~17 days in intermediate blooms of ~30 days duration (see Figure 1c), to ~71 days in long blooms of ~60-day duration (Figure 1d).

In the North Atlantic, phytoplankton typically show a slow growth rate from winter to spring and rapid decline afterward (Mignot et al., 2018). This contrasted temporal variability in the particle production throughout the year is simulated by implementing nonsymmetric Gaussian distributions for the production function (see section 2). In the case of a moderate (i.e., ~45 days) growth and rapid (i.e., ~15 days) decline the duration of the WOS is ~14 days (Figure S3a), while in the opposite case, the case of rapid growth and moderate decline, it lasts ~22 days (Figure S3b).

Our results therefore quantitatively show that the more gradual the onset/decline of the production season is, the longer the sampling periods during which the SS provides consistent results with the directly derived export will extend.

When calculating Th-POC fluxes, we recommend to use these WOS as a reference to determine the accuracy of the SS equations, but they should not be taken as fixed definitive WOS. This is because real bloom are the result of much greater complexity. Indeed, the duration of the WOS is subjected to multiple factors beyond the bloom temporal variability, such as the methodological uncertainties associated to field measurements or spatial variability. Note that the duration of the WOS is not significantly sensitive to the ratio degradation rate/sinking rate (i.e., the main simulated POC flux controller [de Soto et al., 2018]; see Figure S4).

On the other hand, in the case of the NSS approach, a permanent WOS for sampling for an accurate evaluation of the export extends along the entire productive season regardless the bloom duration and intensity for the correct time lag between reoccupations of the sampling site (Figures 1 and S2). We found that the best results for reoccupation times of 2–3 weeks (Figure 1 and S2 of Article 3).

## 4. Implications

Table 1 shows a compilation of several studies that evaluated the POC export using simultaneously sediment traps and the SS-$^{234}$Th technique. We compare the success of assuming SS to calculate the POC flux from $^{234}$Th profiles to estimate the trap-derived POC reported in the North Atlantic by Stewart et al. (2011) at the Bermuda Atlantic Time Series (BATS) station, Le Moigne, Villa-Alfageme, et al. (2013) at the PAP site, and Ceballos-Romero et al. (2016) in both Irminger Basin (IRB) and Iceland Basin (IB) to the predictions of our seasonal studies. In order to correctly refer the WOS to prebloom (postbloom) conditions in the real scenarios of the three cases, we need to introduce a TL between production and export, depending on the sampling area (see section 2). Following Stange et al. (2016), we corrected our DFME with an average factor of

**Table 1**
*Comparison of the Success of Applying the SS Approach to Obtain the Carbon Export From $^{234}$Th Profiles to Estimate the Trap-Derived Export Reported by Several Studies to the Predictions of Our Seasonal Studies (Which Includes Contrasting Sampling Sites and Bloom Stages)*

| Published results | | | This paper |
|---|---|---|---|
| Sampling site and period | Bloom dynamics | Reported POC flux comparison | Predicted POC flux comparison |
| (i) Irminger Basin[a] Jul.–Aug. 2010 | Strong decline of Chl *a* | $^{SS}$POC > POC up to 8 fold | $^{SS}$POC > POC up to threefold[d] |
| (ii) Iceland Basin[a] Jul.–Aug. 2010 | Strong decline of Chl *a* | $^{SS}$POC > POC up to fivefold | $^{SS}$POC > POC up to threefold[d] |
| (iii) PAP Site[b] Jul.–Aug. 2009 | Postbloom | $^{SS}$POC ~ POC | $^{SS}$POC ~ POC[c] |
| (iv) BATS[d] January 2007 | Start of the bloom | $^{SS}$POC ~ POC | $^{SS}$POC ~ POC[e] |
| (v) BATS[d] March 2007 | Bloom | $^{SS}$POC ~ POC | $^{SS}$POC ~ POC[e] |

*Note.* BATS = Bermuda Atlantic Time Series; Chl *a* = chlorophyll *a*; POC = particulate organic carbon; SS = steady state. [a]Ceballos-Romero et al. (2016). [b]Le Moigne, Villa-Alfageme, et al. (2013). [c]Export scenario qualitatively comparable to relatively smooth 45-day blooms (Figure 1c). [d]Stewart et al. (2011). [e]Export scenario qualitatively comparable to our smooth 60-day bloom (Figure S2c). [f]Export scenario qualitatively comparable to our short and intense 15-day bloom (Figure S2a).

−7 days for all the North Atlantic studies. Taking this into account, we find that our predictions are in agreement with the results reported in the literature for both the PAP site and the BATS stations.

For example, at the PAP site, the time gap between the decline of the bloom and the start of sampling was ~34 days (Ceballos-Romero et al., 2016, Figures 4c and 4d), which relative to the DFME of our study of a 45-day bloom, implies that we performed sampling within the WOS and therefore found agreement between PELAGRA and SS-$^{234}$Th. A similar agreement between literature results and our predictions is found for both BATS studies, where both Chl *a* and PP concentrations show very low variability (Villa-Alfageme et al., 2016, Figure 2), and thus, sampling it was always very likely take place during the WOS. This would explain why previous studies have reported good agreement between traps and $^{234}$Th in oligotrophic regions (e.g., Maiti et al., 2016; Owens et al., 2013; Stewart et al., 2011). Therefore, we believe that the SS approach can be successfully applied to $^{234}$Th in midlatitudes between 30°N and 30°S where limited seasonal variability (Cole et al., 2012) likely entails conditions close to SS (Maiti et al., 2016), and field campaigns in these regions (e.g., at station ALOHA in Hawaii or BATS) are likely unaffected when assuming SS in radionuclide concentrations. The NSS provides consistent results with traps and $^{234}$Th-SS-derived POC when sampling along the postpeak phase for blooms with moderate and low (i.e., 45–60 days) temporal variability.

In the case of the North Atlantic (IRB and IB), confronting our predications is more complicated since biochemical conditions in 2010 were atypical in these regions (Ceballos-Romero et al., 2016; Henson et al., 2006, 2013; Ryan-Keogh et al., 2013). Chl *a* concentrations were anomalously high and persisting through autumn 2010 (Ceballos-Romero et al., 2016, Figures 4a and 4b) despite both regions usually present post-bloom conditions during July (Nielsdóttir et al., 2012; Sanders et al., 2005; Waniek & Holliday, 2006). According to our predictions, the SS approach would significantly overestimate the trap-derived export when sampling at the beginning of the postpeak phase in blooms with high temporal variability (i.e., 15 days), and this could explain the discrepancies of an order of magnitude between direct- and SS-POC reported by Ceballos-Romero et al. (2016) in the IRB and IB.

Finally, the uncertainty associated to the Th-POC flux is also related to its spatial variability. Previously, several studies pointed out a significant submesoscale variability of the $^{234}$Th fluxes in some locations. For instance, Buesseler et al. (2009) showed that the $^{234}$Th flux varied over 35–40% on spatial scales of 200–300 km at BATS and K2. Further, Resplandy et al. (2012) reported both measured and modeled variabilities in $^{234}$Th fluxes of about 50% at the PAP site during the D341 cruise (whose results are shown here). Additionally, Estapa et al. (2015) found that $^{234}$Th-derived export fluxes presented a spatial variability at the submesoscale level (~2 km) at BATS likely due to upwelling and horizontal advective fluxes.

Note that in a regional scale, as shown in the seminal work of Resplandy et al. (2012), the uncertainties associated with spatial variability cannot be uncoupled from the uncertainties of assuming SS or NSS. This is applicable to every in situ $^{234}$Th measurements made. If sampling occurs within WOS, one can assume that the spatial variability is then the main source of discrepancy.

The areas mentioned above were clearly associated to SS conditions, with the exception of K2—that is, as all in stable postbloom conditions and within WOS—and confirm the large variability of $^{234}$Th fluxes at the mesoscale and submesoscale level. Because of this, the export fluxes from PAP site, during D341, used in this work were averaged from 10 profiles collected within 100 km. Le Moigne, Villa-Alfageme, et al. (2013) found a variability of $^{234}$Th-derived POC fluxes in the area of 50%, in agreement with Resplandy et al. (2012) model for $^{234}$Th fluxes but also in agreement with the variability from sediment traps deployed in the same area. Since the sampling was performed within WOS, the discrepancies between profiles for $^{234}$Th-derived POC fluxes could be due to the spatial variability of the POC export as predicted by Estapa et al. (2015) for BATS, in agreement with the conclusions from Resplandy et al. (2012).

## 5. Conclusions

With our simplified bloom simulation we are able to predict discrepancies between direct and SS-$^{234}$Th export although the quantification of the actual magnitude of the discrepancies requires a greater complexity in our representation of the bloom. Overall, our predictions suggest that the accuracy of the current available $^{234}$Th-derived estimates of carbon export based on the assumption of the SS should be reevaluated in relation to the WOS presented here.

In future $^{234}$Th studies, we recommend to examine the available information on the main phenomenological events of interest associated with the bloom, which includes bloom timing, and/or peak date, and/or duration, and, when possible, spatial variability, detailed by station to precisely assess the WOS for each station.

**Acknowledgments**
This work was supported by la Caixa (Spain) through a Grant for Graduate Studies (E. C. R.), the Universidad de Sevilla (M. V. A. and E. C. R.), and FIS2015-69673-P project from Spanish MICINN (M. V. A.). The data used are listed in the references, tables, and supplements.

## References

Amiel, D., Cochran, J. K., & Hirschberg, D. J. (2002). U disequilibrium as an indicator of the seasonal export flux of particulate organic carbon in the North Water. *Deep Sea Research, Part II*, *49*(22-23), 5191–5209. Retrieved from https://ac.els-cdn.com/S0967064502001856/1-s2.0-S0967064502001856-main.pdf?_tid=21bf14be-df6f-11e7-b615-00000aacb35d&acdnat=1513105594_78bcbf36b7345b466cdcfd6fe186e5fe. https://doi.org/10.1016/S0967-0645(02)00185-6

Benitez-Nelson, C., Buesseler, K. O., Karl, D. M., & Andrews, J. (2001). A time-series study of particulate matter export in the North Pacific Subtropical Gyre based on 234Th: 238U disequilibrium. *Deep Sea Research Part I: Oceanographic Research Papers*, *48*(12), 2595–2611. https://doi.org/10.1016/S0967-0637(01)00032-2

Buesseler, K. O. (1998). The decoupling of production and particle export in the surface ocean. *Global Biogeochemical Cycles*, *12*(2), 297–310. https://doi.org/10.1029/97GB03366

Buesseler, K. O., Andrews, J. A., Hartman, M. C., Belastock, R., & Chai, F. (1995). Regional estimates of the export flux of particulate organic carbon derived from thorium-234 during the JGOFS EqPac program. *Deep Sea Research Part II: Topical Studies in Oceanography*, *42*(2–3), 777–804. https://doi.org/10.1016/0967-0645(95)00043-P

Buesseler, K. O., Andrews, J. E., Pike, S., Charette, M. A., Buesseler, K. O., A, J. E., P, S. M., et al. (2005). Particle export during the Southern Ocean Iron Experiment (SOFeX). *Limnology and Oceanography*, *50*(1), 311–327. https://doi.org/10.4319/lo.2005.50.1.0311

Buesseler, K. O., Bacon, M. P., Kirk Cochran, J., Livingston, H. D., Cochran, J. K., & Livingston, H. D. (1992). Carbon and nitrogen export during the JGOFS North-Atlantic bloom experiment estimated from Th-234u-238 disequilibria. *Deep-Sea Research Part a-Oceanographic Research Papers*, *39*(7-8), 1115–1137. https://doi.org/10.1016/0198-0149(92)90060-7

Buesseler, K. O., Ball, L., Andrews, J., Benitez-Nelson, C., Belastock, R., Chai, F., & Chao, Y. (1998). Upper ocean export of particulate organic carbon in the Arabian Sea derived from thorium-234. *Deep Sea Research Part II: Topical Studies in Oceanography*, *45*(10–11), 2461–2487. https://doi.org/10.1016/S0967-0645(98)80022-2

Buesseler, K. O., Lamborg, C., Cai, P., Escoube, R., Johnson, R., Pike, S., Masque, P., et al. (2008). Particle fluxes associated with mesoscale eddies in the Sargasso Sea. *Deep Sea Research Part II: Topical Studies in Oceanography*, *55*(10–13), 1426–1444. https://doi.org/10.1016/j.dsr2.2008.02.007

Buesseler, K. O., Lamborg, C. H., Boyd, P. W., Lam, P. J., Trull, T. W., Bidigare, R. R., Bishop, J. K. B., et al. (2007). Revisiting carbon flux through the ocean's twilight zone. *Science*, *316*(5824), 567–570. https://doi.org/10.1126/science.1137959

Buesseler, K. O., Pike, S., Maiti, K., Lamborg, C. H., Siegel, D. A., & Trull, T. W. (2009). Thorium-234 as a tracer of spatial, temporal and vertical variability in particle flux in the North Pacific. *Deep Sea Research Part I: Oceanographic Research Papers*, *56*(7), 1143–1167. Retrieved from http://www.sciencedirect.com/science/article/pii/S0967063709000715, https://doi.org/10.1016/j.dsr.2009.04.001

Buesseler, K. O., Trull, T. W., Steinberg, D. K., Silver, M. W., Siegel, D. A., Saitoh, S. I., Lamborg, C. H., et al. (2008). VERTIGO (VERtical transport in the Global Ocean): A study of particle sources and flux attenuation in the North Pacific. *Deep Sea Research Part II: Topical Studies in Oceanography*, *55*(14–15), 1522–1539. https://doi.org/10.1016/j.dsr2.2008.04.024

Burd, A. B., Hansell, D. A., Steinberg, D. K., Anderson, T. R., Arístegui, J., Baltar, F., Beaupré, S. R., et al. (2010). Assessing the apparent imbalance between geochemical and biochemical indicators of meso- and bathypelagic biological activity: What the @$#! is wrong with present calculations of carbon budgets? *Deep Sea Research Part II: Topical Studies in Oceanography*, *57*(16), 1557–1571. Retrieved from https://www.sciencedirect.com/science/article/pii/S0967064510000883, https://doi.org/10.1016/j.dsr2.2010.02.022

Burd, A. B., Moran, S. B., & Jackson, G. A. (2000). A coupled adsorption-aggregation model of the POC/$^{234}$Th ratio of marine particles. *Deep Sea Research Part I: Oceanographic Research Papers*, *47*(1), 103–120. https://doi.org/10.1016/S0967-0637(99)00047-3

Ceballos-Romero, E., Le Moigne, F. A. C. A. C., Henson, S., Marsay, C. M. M., Sanders, R. J. J., Garcia-Tenorio, R., & Villa-Alfageme, M. (2016). Influence of bloom dynamics on particle export efficiency in the North Atlantic: A comparative study of radioanalytical techniques and sediment traps. *Marine Chemistry*, *186*, 198–210. https://doi.org/10.1016/j.marchem.2016.10.001

Cole, H. S., Henson, S. A., Martin, A. P., & Yool, A. (2012). Mind the gap: The impact of missing data on the calculation of phytoplankton phenology metrics. *Journal of Geophysical Research*, *117*, C08030. https://doi.org/10.1029/2012JC008249

Coppola, L., Roy-Barman, M., Mulsow, S., Povinec, P., & Jeandel, C. (2005). Low particulate organic carbon export in the frontal zone of the Southern Ocean (Indian sector) revealed by $^{234}$Th. *Deep-Sea Research Part I: Oceanographic Research Papers*, *52*(1), 51–68. https://doi.org/10.1016/j.dsr.2004.07.020

de Soto, F., Ceballos-Romero, E., & Villa-Alfageme, M. (2018). A microscopic simulation of particle flux in ocean waters: Application to radioactive pair disequilibrium. *Accepted in Geochimica et Cosmochimica Acta*, *239*, 136–158. https://doi.org/10.1016/J.GCA.2018.07.031

Ducklow, H. W., Steinberg, D., & Buesseler, K. O. (2001). Upper ocean carbon export and the biological pump. *Oceanography*, *14*(4), 50–58. https://doi.org/10.5670/oceanog.2001.06

Estapa, M. L., Siegel, D. A., Buesseler, K. O., Stanley, R. H. R., Lomas, M. W., & Nelson, N. B. (2015). Decoupling of net community and export production on submesoscales in the Sargasso Sea. *Global Biogeochemical Cycles*, *29*, 1266–1282. https://doi.org/10.1002/2014GB004913

Friedrich, J., & Rugters van der Loeff, M. M. (2002). A two-tracer ($^{210}$Po-$^{234}$Th) approach to distinguish organic carbon and biogenic silica export flux in the Antarctic Circumpolar Current. *Deep Sea Research Part I: Oceanographic Research Papers*, *49*(1), 101–120. Retrieved from http://www.sciencedirect.com/science/article/pii/S0967063701000450. https://doi.org/10.1016/S0967-0637(01)00045-0

Giering, S. L. C., Sanders, R., Lampitt, R. S., Anderson, T. R., Tamburini, C., Boutrif, M., Zubkov, M. V., et al. (2014). Reconciliation of the carbon budget in the ocean's twilight zone. *Nature*, *507*(7493), 480–483. https://doi.org/10.1038/nature13123

Gustafsson, Ö., Andersson, P., Roos, P., Kukulska, Z., Broman, D., Larsson, U., Hajdu, S., et al. (2004). Evaluation of the collection efficiency of upper ocean sub-photic-layer sediment traps: A 24-month in situ calibration in the open Baltic Sea using $^{234}$Th. *Limnology and Oceanography: Methods*, *2*(2), 62–74. https://doi.org/10.4319/lom.2004.2.62

Henson, S. A., Painter, S. C., Penny Holliday, N., Stinchcombe, M. C., & Giering, S. L. C. (2013). Unusual subpolar North Atlantic phytoplankton bloom in 2010: Volcanic fertilization or North Atlantic Oscillation? *Journal of Geophysical Research: Oceans*, *118*, 4771–4780. https://doi.org/10.1002/jgrc.20363

Henson, S. A., Robinson, I., Allen, J. T., & Waniek, J. J. (2006). Effect of meteorological conditions on interannual variability in timing and magnitude of the spring bloom in the Irminger Basin, North Atlantic. *Deep Sea Research Part I: Oceanographic Research Papers*, *53*(10), 1601–1615. Retrieved from http://www.sciencedirect.com/science/article/pii/S0967063706002160, https://doi.org/10.1016/j.dsr.2006.07.009

Henson, S. A., Sanders, R., Madsen, E., Morris, P. J., Le Moigne, F. A. C., & Quartlya, G. D. (2011). A reduced estimate of the strength of the ocean's biological carbon pump. *Geophysical Research Letters*, *38*, L04606. Retrieved from http://www.bristol.ac.uk/earthsciences/people/paul-j-morris/pub/9098813, https://doi.org/10.1029/2011GL046735

Henson, S. A., Yool, A., & Sanders, R. (2015). Variability in efficiency of particulate organic carbon export: A model study. *Global Biogeochemical Cycles*, *29*, 33–45. https://doi.org/10.1002/2014GB004965.Received

Jackson, G. A., & Burd, A. B. (2001). A model for the distribution of particle flux in the mid-water column controlled by subsurface biotic interactions. *Deep Sea Research Part II: Topical Studies in Oceanography*, *49*(1-3), 193–217. https://doi.org/10.1016/S0967-0645(01)00100-X

Kriest, I., & Oschlies, A. (2008). On the treatment of particulate organic matter sinking in large-scale models of marine biogeochemical cycles. *Biogeosciences*, *5*(1), 55–72. Retrieved from www.biogeosciences.net/5/55/2008/, https://doi.org/10.5194/bg-5-55-2008

Kwon, E. Y., Primeau, F., & Sarmiento, J. L. (2009). The impact of remineralization depth on the air-sea carbon balance. *Nature Geoscience*, *2*(9), 630–635. https://doi.org/10.1038/ngeo612

Lamborg, C. H., Buesseler, K. O., Valdes, J., Bertrand, C. H., Bidigare, R., Manganini, S., Pike, S., et al. (2008). The flux of bio- and lithogenic material associated with sinking particles in the mesopelagic "twilight zone" of the northwest and North Central Pacific Ocean. *Deep Sea Research Part II: Topical Studies in Oceanography*, *55*(14–15), 1540–1563. https://doi.org/10.1016/j.dsr2.2008.04.011

Lampitt, R. S., Boorman, B., Brown, L., Lucas, M., Salter, I., Sanders, R., Saw, K., et al. (2008). Particle export from the euphotic zone: Estimates using a novel drifting sediment trap, $^{234}$Th and new production. *Deep Sea Research Part I: Oceanographic Research Papers*, *55*(11), 1484–1502. Retrieved from http://www.sciencedirect.com/science/article/pii/S0967063708001453, https://doi.org/10.1016/j.dsr.2008.07.002

Le Moigne, F. A. C., Henson, S. A., Cavan, E., Georges, C., Pabortsava, K., Achterberg, E. P., Ceballos-Romero, E., et al. (2016). What causes the inverse relationship between primary production and export efficiency in the Southern Ocean? *Geophysical Research Letters*, *43*, 4457–4466. https://doi.org/10.1002/2016GL068480

Le Moigne, F. A. C., Henson, S. A., Sanders, R. J., & Madsen, E. (2013). Global database of surface ocean particulate organic carbon export fluxes diagnosed from the $^{234}$Th technique. *Earth System Science Data*, *5*(2), 295–304. https://doi.org/10.1594/PANGAEA.809717

Le Moigne, F. A. C., Poulton, A. J., Henson, S. A., Daniels, C. J., Fragoso, G. M., Mitchell, E., Richier, S., et al. (2015). Carbon export efficiency and phytoplankton community composition in the Atlantic sector of the Arctic Ocean. *Journal of Geophysical Research: Oceans*, *120*, 3896–3912. https://doi.org/10.1002/2015JC010700

Le Moigne, F. A. C., Villa-Alfageme, M., Sanders, R. J., Marsay, C., Henson, S., & García-Tenorio, R. (2013). Export of organic carbon and biominerals derived from $^{234}$Th and $^{210}$Po at the Porcupine Abyssal Plain. *Deep Sea Research Part I: Oceanographic Research Papers*, *72*(0), 88–101. Retrieved from http://www.sciencedirect.com/science/article/pii/S0967063712002075, https://doi.org/10.1016/j.dsr.2012.10.010

Maiti, K., Benitez-Nelson, C. R., Lomas, M. W., & Krause, J. W. (2009). Biogeochemical responses to late-winter storms in the Sargasso Sea, III—Estimates of export production using 234Th:238U disequilibria and sediment traps. *Deep Sea Research Part I: Oceanographic Research Papers*, *56*(6), 875–891. Retrieved from http://www.sciencedirect.com/science/article/pii/S0967063709000284, https://doi.org/10.1016/j.dsr.2009.01.008

Maiti, K., Benitez-Nelson, C. R., Rii, Y., & Bidigare, R. (2008). The influence of a mature cyclonic eddy on particle export in the lee of Hawaii. *Deep-Sea Research Part II: Topical Studies in Oceanography*, *55*(10–13), 1445–1460. https://doi.org/10.1016/j.dsr2.2008.02.008

Maiti, K., Bosu, S., D'Sa, E. J. J., Adhikari, P. L. L., Sutor, M., & Longnecker, K. (2016). Export fluxes in northern Gulf of Mexico—Comparative evaluation of direct, indirect and satellite-based estimates. *Marine Chemistry*, *184*, 60–77. https://doi.org/10.1016/j.marchem.2016.06.001

Marchal, O., & Lam, P. J. (2012). What can paired measurements of Th isotope activity and particle concentration tell us about particle cycling in the ocean? *Geochimica et Cosmochimica Acta*, *90*, 126–148. https://doi.org/10.1016/j.gca.2012.05.009

Marsay, C. M., Sanders, R. J., Henson, S. A., Pabortsava, K., Achterberg, E. P., & Lampitt, R. S. (2015). Attenuation of sinking particulate organic carbon flux through the mesopelagic ocean. *Proceedings of the National Academy of Sciences*, *112*(4), 1089–1094. Retrieved from http://www.pnas.org/content/112/4/1089.abstract

Mignot, A., Ferrari, R., & Claustre, H. (2018). Floats with bio-optical sensors reveal what processes trigger the North Atlantic bloom. *Nature Communications*, *9*(1), 190. https://doi.org/10.1038/s41467-017-02143-6

Morris, P. J., Sanders, R., Robert, T., Sandy, T., Turnewitsch, R., & Thomalla, S. (2007). $^{234}$Th-derived particulate organic carbon export from an island-induced phytoplankton bloom in the Southern Ocean. *Deep-Sea Research Part II*, *54*(18–20), 2208–2232. https://doi.org/10.1016/j.dsr2.2007.06.002

Nielsdóttir, M. C., Bibby, T. S., Moore, C. M., Hinz, D. J., Sanders, R., Whitehouse, M., Korb, R., et al. (2012). Seasonal and spatial dynamics of iron availability in the Scotia Sea. *Marine Chemistry*, *130-131*(0), 62–72. https://doi.org/10.1016/j.marchem.2011.12.004

Owens, S. A., Buesseler, K. O., Lamborg, C. H., Valdes, J., Lomas, M. W., Johnson, R. J., Steinberg, D. K., et al. (2013). A new time series of particle export from neutrally buoyant sediments traps at the Bermuda Atlantic Time-series Study site. *Deep Sea Research Part I: Oceanographic Research Papers*, *72*, 34–47. https://doi.org/10.1016/j.dsr.2012.10.011

Owens, S. A., Buesseler, K. O., & Sims, K. W. W. (2011). Re-evaluating the $^{238}$U-salinity relationship in seawater: Implications for the $^{238}$U/$^{234}$Th disequilibrium method. *Marine Chemistry*, *127*(1–4), 31–39. Retrieved from http://www.sciencedirect.com/science/article/pii/S030442031100082X, https://doi.org/10.1016/j.marchem.2011.07.005

Owens, S. A., Pike, S., & Buesseler, K. O. (2015). Thorium-234 as a tracer of particle dynamics and upper ocean export in the Atlantic Ocean. *Deep Sea Research Part II: Topical Studies in Oceanography*, *116*(0), 42–59. https://doi.org/10.1016/j.dsr2.2014.11.010

Passow, U., Dunne, J., Murray, J. W., Balistrieri, L., & Alldredge, A. L. (2006). Organic carbon to $^{234}$Th ratios of marine organic matter. *Marine Chemistry*, *100*(3-4), 323–336. https://doi.org/10.1016/j.marchem.2005.10.020

Planchon, F., Ballas, D., Cavagna, A. J., Bowie, A. R., Davies, D., Trull, T., Laurenceau-Cornec, E. C., et al. (2015). Carbon export in the naturally iron-fertilized Kerguelen area of the Southern Ocean based on the $^{234}$Th approach. *Biogeosciences*, *12*(12), 3831–3848. https://doi.org/10.5194/bg-12-3831-2015

Puigcorbé, V., Roca-Martí, M., Masqué, P., Benitez-Nelson, C. R., ven der Loeff, M. R., Laglera, L. M., Bracher, A., et al. (2017). Particulate organic carbon export across the Antarctic Circumpolar Current at 10°E: Differences between north and south of the Antarctic Polar Front. *Deep Sea Research Part II: Topical Studies in Oceanography*, *138*, 86–101. https://doi.org/10.1016/J.DSR2.2016.05.016

Resplandy, L., Martin, A. P., Le Moigne, F., Martin, P., Aquilina, A., Mémery, L., Lévy, M., et al. (2012). How does dynamical spatial variability impact 234Th-derived estimates of organic export? *Deep Sea Research Part I: Oceanographic Research Papers*, *68*(0), 24–45. Retrieved from http://resplandy201224.html, https://doi.org/10.1016/j.dsr.2012.05.015

Riley, J. S., Sanders, R., Marsay, C., Moigne, F. A. C., Le Achterberg, E. P., & Poulton, A. J. (2012). The relative contribution of fast and slow sinking particles to ocean carbon export. *Global Biogeochemical Cycles*, *26*, GB1026. https://doi.org/10.1029/2011GB004085

Roca-Martí, M., Puigcorbé, V., Iversen, M. H., van der Loeff, M. R., Klaas, C., Cheah, W., Bracher, A., et al. (2015). High particulate organic carbon export during the decline of a vast diatom bloom in the Atlantic sector of the Southern Ocean. *Deep Sea Research Part II: Topical Studies in Oceanography*. https://doi.org/10.1016/j.dsr2.2015.12.007

Rosengard, S. Z., Lam, P. J., Balch, W. M., Auro, M. E., Pike, S., Drapeau, D., & Bowler, B. (2015). Carbon export and transfer to depth across the Southern Ocean Great Calcite Belt. *Biogeosciences*, *12*(13), 3953–3971. https://doi.org/10.5194/bg-12-3953-2015

Rutgers van der Loeff, M., Friedrich, J., & Bathmann, U. V. (1997). Carbon export during the Spring Bloom at the Antarctic Polar Front, determined with the natural tracer $^{234}$Th. *Deep-Sea Research II3*, *44*(1-2), 457–478. Retrieved from https://ac.els-cdn.com/S0967064596000677/1-s2.0-S0967064596000677-main.pdf?_tid=9a4cb140-e003-11e7-aebd-00000aab0f6c&acdnat=1513169354_e25fd5bbdc655568d577a4ba570e9ddb, https://doi.org/10.1016/S0967-0645(96)00067-7

Ryan-Keogh, T. J., Macey, A. I., Nielsdóttir, M. C., Lucas, M. I., Steigenberger, S. S., Stinchcombe, M. C., Achterberg, E. P., et al. (2013). Spatial and temporal development of phytoplankton iron stress in relation to bloom dynamics in the high-latitude North Atlantic Ocean. *Limnology and Oceanography*, *58*(2), 533–545. https://doi.org/10.4319/lo.2013.58.2.0533

Sanders, R., Brown, L., Henson, S., & Lucas, M. (2005). New production in the Irminger Basin during 2002. *Journal of Marine Systems*, *55*(3–4), 291–310. Retrieved from http://www.sciencedirect.com/science/article/pii/S092479630400260X, https://doi.org/10.1016/j.jmarsys.2004.09.002

Savoye, N., Benitez-Nelson, C., Burd, A. B., Cochran, J. K., Charette, M., Buesseler, K. O., Jackson, G. A., et al. (2006). $^{234}$Th sorption and export models in the water column: A review. *Marine Chemistry*, *100*(3–4), 234–249. Retrieved from http://www.sciencedirect.com/science/article/pii/S030442030500215X, https://doi.org/10.1016/j.marchem.2005.10.014

Savoye, N., Buesseler, K. O., Cardinal, D., & Dehairs, F. (2004). $^{234}$Th deficit and excess in the Southern Ocean during spring 2001: Particle export and remineralization. *Geophysical Research Letters*, *31*, L12301. https://doi.org/10.1029/2004GL019744

Stange, P., Bach, L. T., Le Moigne, F. A. C., Taucher, J., Boxhammer, T., & Riebesell, U. (2016). Quantifying the time lag between organic matter production and export in the surface ocean: Implications for estimates of export efficiency. *Geophysical Research Letters*, *44*, 268–276. https://doi.org/10.1002/2016GL070875

Stewart, G., Cochran, J. K., Miquel, J. C., Masqué, P., Szlosek, J., Rodriguez y Baena, A. M., Fowler, S. W., et al. (2007). Comparing POC export from $^{234}$Th/$^{238}$U and $^{210}$Po/$^{210}$Pb disequilibria with estimates from sediment traps in the northwest Mediterranean. *Deep Sea Research Part I: Oceanographic Research Papers*, *54*(9), 1549–1570. https://doi.org/10.1016/j.dsr.2007.06.005

Stewart, G., Cochran, J. K., Xue, J., Lee, C., Wakeham, S. G., Armstrong, R. A., Masqué, P., et al. (2007). Exploring the connection between $^{210}$Po and organic matter in the northwestern Mediterranean. *Deep Sea Research Part I: Oceanographic Research Papers*, *54*(3), 415–427. Retrieved from http://www.sciencedirect.com/science/article/pii/S0967063706003311, https://doi.org/10.1016/j.dsr.2006.12.006

Stewart, G., Moran, S. B., Lomas, M. W., & Kelly, R. P. (2011). Direct comparison of 210Po, 234Th and POC particle-size distributions and export fluxes at the Bermuda Atlantic Time-series Study (BATS) site. *Journal of Environmental Radioactivity*, *102*(5), 479–489. https://doi.org/10.1016/j.jenvrad.2010.09.011

Stukel, M. R., Asher, E., Couto, N., Schofield, O., Strebel, S., Tortell, P., & Ducklow, H. W. (2015). The imbalance of new and export production in the western Antarctic Peninsula, a potentially "leaky" ecosystem. *Global Biogeochemical Cycles*, *29*, 1400–1420. https://doi.org/10.1002/2015GB005211

Verdeny, E., Masqué, P., Garcia-Orellana, J., Hanfland, C., Cochran, J. K., & Stewart, G. M. (2009). POC export from ocean surface waters by means of $^{234}$Th/$^{238}$U and $^{210}$Po/$^{210}$Pb disequilibria: A review of the use of two radiotracer pairs. *Deep Sea Research Part II: Topical Studies in Oceanography*, *56*(18), 1502–1518. Retrieved from http://www.sciencedirect.com/science/article/pii/S0967064508004414, https://doi.org/10.1016/j.dsr2.2008.12.018

Villa-Alfageme, M., de Soto, F., Le Moigne, F. A. C., Giering, S. L. C., Sanders, R., & García-Tenorio, R. (2014). Observations and modeling of slow-sinking particles in the twilight zone. *Global Biogeochemical Cycles*, *28*, 1327–1342. https://doi.org/10.1002/2014GB004981

Villa-Alfageme, M., de Soto, F. C., Ceballos, E., Giering, S. L. C., Le Moigne, F. A. C., Henson, S. A., & Sanders, R. J. (2016). Geographical, seasonal, and depth variation in sinking particle speeds in the North Atlantic. *Geophysical Research Letters*, *43*, 8609–8616. https://doi.org/10.1002/2016GL069233

Volk, T., & Hoffert, M. I. (1985). Ocean carbon pumps: Analysis of relative strengths and efficiencies in ocean-driven atmospheric CO2 changes. In *The carbon cycle and atmospheric CO* (pp. 99–110). Washington, DC: American Geophysical Union. https://doi.org/10.1029/GM032p0099

Waniek, J. J., & Holliday, N. P. (2006). Large-scale physical controls on phytoplankton growth in the Irminger Sea, Part II: Model study of the physical and meteorological preconditioning. *Journal of Marine Systems*, *59*(3–4), 219–237. https://doi.org/10.1016/j.jmarsys.2005.10.005

Wei, C. L., & Murray, J. W. (1992). Temporal variations of $^{234}$Th activity in the water column of Dabob Bay: Particle scavenging. *Limnology and Oceanography*, *37*(2), 296–314. https://doi.org/10.4319/lo.1992.37.2.0296